

Formation of the cerium orthovanadate CeVO_4 : DFT+ U study

Juarez L. F. Da Silva,* M. Verónica Ganduglia-Pirovano,[†] and Joachim Sauer[‡]

Institut für Chemie, Humboldt-Universität zu Berlin, Unter den Linden 6, D-10099 Berlin, Germany

(Received 18 April 2007; revised manuscript received 25 July 2007; published 27 September 2007)

We report density functional theory calculations of the structural, electronic, and thermodynamic properties of cerium orthovanadate (CeVO_4) employing the local density approximation (LDA), generalized gradient approximation (GGA-PBE), LDA+ U , and GGA-PBE+ U functionals. The LDA+ U , GGA-PBE+ U , LDA, and GGA-PBE equilibrium volumes deviate by -2.4% , $+3.6\%$, -7.4% , and -0.8% , respectively, from experimental results. DFT+ U (DFT) predicts an antiferromagnetic (ferromagnetic) insulating (metallic) ground state, which is in agreement with experimental observations. DFT+ U yields Ce and V ions in the III+ and V+ oxidation state, respectively. CeVO_4 can be obtained by the reaction between Ce_2O_3 and V_2O_5 [$\frac{1}{2}\text{Ce}_2\text{O}_3(\text{s}) + \frac{1}{2}\text{V}_2\text{O}_5(\text{s}) \rightarrow \text{CeVO}_4(\text{s})$] under an inert atmosphere, which is described as exoenergetic ($|\Delta H_0| = 1.6\text{--}1.8\text{ eV}$) by all functionals. The reaction $\frac{1}{2}\text{Ce}_2\text{O}_3(\text{s}) + \frac{1}{2}\text{V}_2\text{O}_5(\text{s}) \rightarrow \text{CeO}_2(\text{s}) + \text{VO}_2(\text{s})$ is exoenergetic with $|\Delta H_0| = 0.75, 0.25, 1.70,$ and 1.24 eV for LDA+ U , GGA-PBE+ U , LDA, and GGA-PBE, respectively. Hence, V^{V+} is more easily reduced to $\text{V}^{\text{IV+}}$ than $\text{Ce}^{\text{IV+}}$ to $\text{Ce}^{\text{III+}}$, but the difference is small as obtained with DFT+ U , PBE+ U , in particular. The variation of this reaction energy is due to the different performance of the various approaches for the description of the change in oxidation state of cerium, IV+ to III+ [J. L. F. Da Silva *et al.*, Phys. Rev. B **75**, 045121 (2007)]. The small difference between the V^{V} and Ce^{IV} reducibilities may have consequences for the use of CeO_2 as support of V_2O_5 catalysts in selective oxidation.

DOI: 10.1103/PhysRevB.76.125117

PACS number(s): 71.15.Mb, 74.25.Bt

I. INTRODUCTION

Several reactions are heterogeneously catalyzed by vanadium oxides.¹ Although unsupported vanadia is an active catalyst, supported vanadium oxides are widely used. Activity, selectivity, and stability of such catalysts can be modified by varying the support.²⁻⁴ Among the different supports, e.g., ZrO_2 , TiO_2 , Al_2O_3 , SiO_2 , CeO_2 , and Nb_2O_5 , ceria shows a significant promoting effect. Hence, much effort has been directed toward characterizing vanadia and/or ceria catalysts (see, e.g., Refs. 5-9).

In situ spectroscopic studies of $\text{V}_2\text{O}_5/\text{CeO}_2$ catalysts show clear indications that cerium orthovanadate (CeVO_4) forms upon calcination and its abundance rising in proportion to the vanadia loading on the CeO_2 support.⁷⁻⁹ CeVO_4 is also present in *used* $\text{V}_2\text{O}_5/\text{CeO}_2$ catalysts for oxidative dehydrogenation reactions and is associated with some loss of activity.^{7,9} As vanadia coverage increases, the product distribution for $\text{V}_2\text{O}_5/\text{CeO}_2$ and for pure CeVO_4 catalysts are quite similar. These results indicate that the same active site may be present on both catalysts, and the question of the nature of the Ce-O-V bonds in CeVO_4 is particularly relevant.

The formation of CeVO_4 is also of importance in the functioning of gas turbines. The burning of low-quality fuels, i.e., containing, for example, vanadium impurities, has a corrosive effect on the ceria-stabilized zirconia ceramics used as blade coatings while removing the stabilizer from zirconia and forming CeVO_4 .¹⁰ In addition, CeVO_4 has attracted attention due to its potential applications as a counterelectrode in electrochromic windows,^{11,12} gas sensors, and components of solid oxide fuel cells.¹³

CeVO_4 can be synthesized by solid state reactions between cerium compounds and V_2O_5 . The reaction between cerium oxides with Ce in the III+ oxidation state (Ce_2O_3)

and V_2O_5 is represented by $\frac{1}{2}\text{Ce}_2\text{O}_3(\text{s}) + \frac{1}{2}\text{V}_2\text{O}_5(\text{s}) \rightarrow \text{CeVO}_4(\text{s})$, which requires an inert atmosphere due to the instability of the $\text{Ce}^{\text{III+}}$ compounds in air at high temperatures.¹⁴ Furthermore, CeVO_4 can also be prepared by the conventional solid state reaction of CeO_2 with Ce in the IV+ oxidation state and V_2O_5 in air, i.e., $\text{CeO}_2(\text{s}) + \frac{1}{2}\text{V}_2\text{O}_5(\text{s}) \rightarrow \text{CeVO}_4(\text{s}) + \frac{1}{4}\text{O}_2(\text{g})$.^{15,16} In both reactions, (s) and (g) indicate solid and gas phases, respectively. Furthermore, aiming at controlling the size of the synthesized CeVO_4 particles, different techniques such as the sol-gel route,¹² microwave irradiation processing,¹⁷ and hydrothermal methods¹⁸ have been used.

As mentioned above, the Ce atoms are in the III+ and IV+ oxidation states in the CeO_2 and Ce_2O_3 oxides, respectively.¹⁹ Because also vanadium exhibits multiple valences, the cerium oxidation state in CeVO_4 is not obvious. X-ray absorption spectra indicated that the oxidation state of Ce atoms in CeVO_4 is $\text{Ce}^{\text{III+}}$.²⁰ It was further found that it was possible to create $\text{Ce}^{\text{IV+}}$ by adding persulfate as an oxidant. This implies that cerium is reduced during the solid state reaction of CeO_2 and V_2O_5 and that vanadium remains in the $\text{V}^{\text{V+}}$ oxidation state. So far, CeVO_4 has only been studied by means of a DV- X_α embedded cluster ($\text{CeV}_2\text{O}_{10}$) with frozen geometry calculation.²¹

The determination of the electronic structure of CeVO_4 appears desirable, and it can also provide useful information leading to a better understanding of ceria supported vanadia systems. Therefore, in the present work, we report a theoretical investigation of the structural, electronic, and magnetic properties of bulk CeVO_4 and discuss the cerium and vanadium oxidation states. Furthermore, we present results for the CeVO_4 atomization energy, heat of formation, and reaction energies for solid state reactions yielding CeVO_4 . As required for the evaluation of the thermodynamic properties, calculations were also performed for V_2O_5 , while the total

energies of the CeO_2 , Ce_2O_3 , and O_2 systems were calculated using the equilibrium parameters reported in Ref. 22 (see the Appendix).

II. THEORETICAL APPROACH AND COMPUTATIONAL DETAILS

It is known that density functional theory^{23,24} (DFT) within the local density approximation²⁵ (LDA) or the generalized gradient approximation²⁶ (GGA) often yields qualitatively *incorrect* results for f electron systems in which the f orbital overlaps are small, the f bands narrow, and the f electrons nearly localized.²⁷ For example, DFT-LDA/GGA calculations yield a ferromagnetic (FM) metallic ground state for Ce_2O_3 , which is in contrast with experimental observations, i.e., Ce_2O_3 is an antiferromagnetic (AFM) insulator. This particular discrepancy is due to the localized behavior of the Ce $4f$ states ($\text{Ce}^{\text{III}+}$) in Ce_2O_3 , which is incorrectly described by DFT-LDA/GGA. However, DFT-LDA/GGA yields the correct ground state (nonmagnetic insulator) for CeO_2 due to the delocalized nature of the Ce $4f$ states ($\text{Ce}^{\text{IV}+}$) in CeO_2 .²² The correct ground state for Ce_2O_3 has been obtained by DFT+ U (Refs. 22, 28, and 29) and DFT with hybrid functionals.²² There is not firm evidence for either the localized or the delocalized character of the Ce $4f$ states in CeVO_4 , which is crucial to determine the oxidation state of the Ce atoms. Therefore, calculations employing both DFT and DFT+ U have been performed in the present work.

The implementation of the DFT+ U method, the underlying functional (LDA or GGA), in particular, has been found to have some influence in the description of cerium compounds with $\text{Ce}^{\text{III}+}$ ions (see, e.g., Ref. 30). Hence, both LDA+ U and GGA+ U functionals are considered and discussed. V_2O_5 , however, is described using plain DFT only. Mainly because DFT+ U calculations of reaction energies for solid state reactions yielding CeVO_4 requires the total energy of V_2O_5 , both LDA and GGA (PBE formulation, see Ref. 26) calculations of V_2O_5 are performed.

In DFT+ U , a Hubbard U term corresponding to the mean-field approximation of the on-site Coulomb interaction is added to the LDA or GGA-PBE functionals. The rotationally invariant approach proposed by Dudarev *et al.*³¹ was employed, where an effective parameter $U_{\text{eff}}=U-J$ is introduced. U and J are the Coulomb and exchange parameters, respectively. The Hubbard term was added only to the Ce $4f$ states in the CeVO_4 , CeO_2 , and Ce_2O_3 systems, and values of 5.30 and 4.50 eV were used in the LDA+ U and GGA-PBE+ U calculations, respectively. These values were calculated self-consistently by Fabris *et al.*³² using the linear-response approach of Cococcioni and de Gironcoli,³³ and they were employed in previous calculations on CeO_2 and Ce_2O_3 .^{22,32}

The Kohn-Sham equations were solved using the projected augmented wave (PAW) method,^{34–36} as implemented in the Vienna *ab initio* simulation package (VASP).^{37,38} In the PAW method, the interaction between the ions and electrons are described by the standard frozen-core potentials provided with the VASP package, which were generated according to

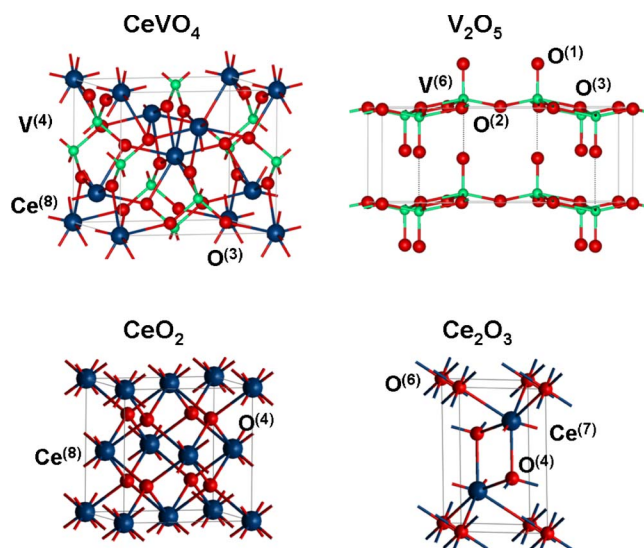


FIG. 1. (Color online) Bulk structures of CeVO_4 , CeO_2 , Ce_2O_3 , and V_2O_5 . The Ce, V, and O atoms are indicated with their coordination as a superscript in parentheses. The dotted lines in the V_2O_5 structure indicate the weak bond between the V_2O_5 crystal layers.

the procedure outlined in Ref. 35. For Ce, V, and O atoms, the ($5s, 5p, 6s, 4f, 5d$), ($3s, 3p, 4s, 3d$), and ($2s, 2p$) electrons were treated as valence, respectively, while the remaining electrons were kept frozen in the core. A plane-wave cutoff energy of 400 eV was chosen for all calculations, except for the stress tensor calculations for which we used a cutoff energy of 800 eV due to the slow convergence of the stress tensor with the number of basis functions. The augmentation charges were evaluated using an additional grid, which contained eight times more points than the grid for the wave functions determined from the cutoff energy. The projection operators were evaluated in reciprocal space.

The Brillouin-zone integrations were performed using Monkhorst-Pack grids,³⁹ namely, ($6 \times 6 \times 6$) and ($2 \times 6 \times 6$) for CeVO_4 and V_2O_5 , respectively. The equilibrium volumes V_0 were calculated by minimizing the stress tensor and all internal degrees of freedom. The bulk moduli B_0 were obtained by fitting the calculated total ground-state energies for 13 relaxed structures with fixed volumes to Murnaghan's equation of state.⁴⁰ All atom positions were relaxed until the forces were smaller than $0.01 \text{ eV}/\text{\AA}$.

III. RESULTS AND DISCUSSION

A. Equilibrium volumes and bulk modulus

CeVO_4 has two polymorphs. The stable phase has a zircon-type body-centered-tetragonal structure with space group $D_{4h}^{19}-I4_1/amd$,^{12,41} whereas the metastable one (stable above 400°C) has a monoclinic huttonite-type structure ($C_{2h}^5-P2_1/n$).¹⁵ We consider only the zircon-type structure. The conventional zircon-type unit cell, as shown in Fig. 1, has 4 f.u., whereas the primitive unit cell used in the actual calculations has 2 f.u. The Ce and V atoms are located at $(0, 3/4, 1/8)$ and $(0, 3/4, 5/8)$ on the $4a$ and $4b$ Wyckoff sites, respectively. The O atoms occupy the $16h$ Wyckoff

TABLE I. Bulk properties of CeVO₄. Equilibrium lattice constants, a_0 and c_0 (in Å), oxygen internal parameters (u_O and v_O), nearest-neighbor distances (in Å), bulk modulus, B_0 (in Mbar), and total magnetic moment in μ_B per primitive unit cell, m (per cerium atom in parentheses). FM and AF indicate ferromagnetic and antiferromagnetic spin configurations, respectively.

	Spin	a_0	c_0	u_O	v_O	Ce-O	Ce-O	V-O	B_0	m
LDA+ U	FM	7.35	6.43	0.0708	0.2053	2.41	2.50	1.71		2.00 (0.96)
LDA+ U	AF	7.35	6.43	0.0708	0.2053	2.41	2.50	1.71	1.20	0.00 (0.96)
GGA-PBE+ U	FM	7.51	6.54	0.0720	0.2066	2.48	2.55	1.73		2.00 (0.96)
GGA-PBE+ U	AF	7.51	6.54	0.0721	0.2065	2.48	2.55	1.73	0.92	0.00 (0.96)
LDA	FM	7.20	6.36	0.0668	0.2008	2.33	2.46	1.72	1.26	2.00 (0.70)
LDA	AF	7.20	6.37	0.0664	0.2010	2.33	2.46	1.72		0.00 (0.43)
GGA-PBE	FM	7.37	6.50	0.0687	0.2025	2.40	2.51	1.74	0.90	2.00 (0.76)
GGA-PBE	AF	7.36	6.49	0.0682	0.2029	2.40	2.52	1.74		0.00 (0.65)
Expt. ^a		7.35	6.49	0.0716	0.2067	2.43	2.52	1.71		
Expt. ^{b,c}		7.40	6.50							

^aReference 41; x-ray diffraction (XRD) of Ce(V_{0.92}As_{0.08})O₄.

^bReference 16; XRD of polycrystalline CeVO₄.

^cReference 13; XRD of single-phase powders of CeVO₄.

sites ($0, u_O, v_O$), where u_O and v_O are internal parameters. Thus, four parameters (a_0, b_0, u_O , and v_O) determine the complete CeVO₄ structure, namely, all atomic positions in the supercell and the equilibrium volume V_0 . The Ce, V, and O atoms are eight-, four-, and threefold coordinated, respectively. The eight O nearest neighbors of Ce are divided in two groups of four atoms each, between which the bond lengths differ slightly (0.09–0.13 Å).

The calculated structural properties are shown in Table I. The available experimental lattice parameters of CeVO₄ have been determined by means of x-ray (powder) diffraction;^{13,16,41} (XRD) however the internal parameters, which determine the oxygen atomic positions, are reported only in Ref. 41. The composition of the sample used in Ref. 41 did not correspond to pure CeVO₄ but to Ce(V_{0.92}As_{0.08})O₄.

The equilibrium volume of CeVO₄, which corresponds to the AFM compound with LDA+ U and GGA-PBE+ U and to the ferromagnetic (FM) one with LDA and GGA-PBE, deviates by -2.4% (LDA+ U), $+3.6\%$ (GGA-PBE+ U), -7.4% (LDA), and -0.8% (GGA-PBE) with respect to most recent experiments.^{13,16} The LDA value is far from being satisfactory, and that obtained using GGA-PBE does not reflect the overestimation expected for GGA functionals.^{42,43} This is in line with recent results for Ce₂O₃ for which the equilibrium volume is underestimated by 8.9% (LDA) and 2.7% (GGA-PBE)²² and provides a hint that the description of the electronic structure using the LDA and GGA-PBE functionals might not be correct, as in the case of Ce₂O₃.

For DFT+ U , the equilibrium volume depends significantly on the description of the plain DFT part (LDA versus GGA-PBE). The inclusion of the Hubbard U term to LDA and GGA-PBE increases the volume of CeVO₄ by about 5% and 3%, respectively. Hence, LDA+ U yields an equilibrium volume closer to the experimental result than the GGA-PBE+ U functional. This is again similar to the description of Ce₂O₃ with a volume increase by up to 6% with the inclusion of U ; however, the volume of CeO₂ changes

only slightly ($\approx 2\%$).²² Also, for the internal parameters u_O and v_O , the LDA+ U results are in better agreement with the experimental values⁴¹ than the GGA-PBE+ U results. Thus, the LDA+ U yielded the best description of the lattice and internal parameters for CeVO₄.

Incorporation of a Hubbard U term acting only on the Ce 4*f* states increases the Ce-O bond lengths by up to 0.08 Å, but the V-O bond by 0.01 Å only. This result once more resembles the description of Ce₂O₃ with an increase of the average Ce-O bond length by 0.05 Å on inclusion of U , which is a reflection of the localization of the Ce 4*f* states by the DFT+ U approach.²²

Furthermore, the average experimental Ce-O bond length of the eightfold coordinated Ce atoms in CeVO₄ of 2.48 Å (4×2.43 and 4×2.52 Å) is closer to the value of 2.50 Å in Ce₂O₃ than to the 2.34 Å in CeO₂. In CeO₂, the Ce atoms are eightfold coordinated with a Ce-O bond length of 2.34 Å,^{44–47} whereas in Ce₂O₃, the Ce atoms are sevenfold coordinated with Ce-O bond lengths of 3×2.34 , 1×2.43 , and 3×2.69 Å.^{48,49} The increase in Ce-O bond lengths from CeO₂ to Ce₂O₃ accompanies the change in the oxidation state from Ce^{IV+} to Ce^{III+}.²² Hence, the similarity of the average Ce-O bond length in CeVO₄ and Ce₂O₃ might be taken as indication that Ce^{III+} is present in both compounds.

Vanadium pentoxide is a nonmagnetic layered system with a soft direction perpendicular to the V₂O₅ layers (see Fig. 1). Strong covalent bonding occur between the V and O atoms in the layers, whereas weak van der Waals (vdW) interactions exist between the layers. V₂O₅ has an orthorhombic structure with space group D_{2h}^{13} - $Pmmn$.⁵⁰ The primitive unit cell comprises 2 f.u. with four crystallographically inequivalent atoms, one vanadium and three oxygen atoms. The oxygen atoms, usually denoted O⁽¹⁾, O⁽²⁾, and O⁽³⁾, have different coordination. The vanadyl oxygen O⁽¹⁾, the bridging oxygen O⁽²⁾, and the O⁽³⁾ oxygen atoms are one-, two-, and threefold coordinated, respectively (see Fig. 1). Vanadium is coordinated to five oxygen atoms within a layer (O⁽¹⁾, O⁽²⁾, $3 \times O^{(3)}$), and there is a weak coordination to the O⁽¹⁾ oxygen of the layer beneath.

TABLE II. Bulk properties of V_2O_5 . Equilibrium lattice constants, a_0 , b_0 , and c_0 (in \AA), nearest-neighbor distances (in \AA), bulk modulus, B_0 (in Mbar), and V and O atom positions. The Wyckoff positions are given in brackets.

	a_0	b_0	c_0	V-O ⁽¹⁾	V-O ⁽²⁾	V-O ⁽³⁾	V-O ^(3')	V...O ⁽¹⁾	B_0
LDA	11.70	3.54	3.93	1.61	1.77	1.85	2.03	2.32	0.70
GGA-PBE	11.56	3.58	4.86	1.60	1.79	1.89	2.04	3.26	0.08
Expt. ^a	11.51	3.56	4.37	1.58	1.78	1.88	2.02	2.79	
	V [4f] (x,y,z)			O ⁽¹⁾ [4f] (x,y,z)		O ⁽²⁾ [2a] (x,y,z)		O ⁽³⁾ [4f] (x,y,z)	
LDA	(0.1021, 1/4, 0.8999)			(0.1013, 1/4, 0.4908)		(1/4, 1/4, -0.0113)		(-0.0676, 1/4, 0.0032)	
GGA-PBE	(0.1016, 1/4, 0.8906)			(0.1061, 1/4, 0.5619)		(1/4, 1/4, -0.0009)		(-0.0683, 1/4, 0.0082)	
Expt. ^a	(0.1011, 1/4, 0.8917)			(0.1043, 1/4, 0.5310)		(1/4, 1/4, +0.0010)		(-0.0689, 1/4, 0.0030)	

^aReference 50.

Table II shows the optimized lattice parameters, a_0 , b_0 , and c_0 , and the fractional coordinates using the LDA and GGA-PBE functionals and compares them with experiment.⁵⁰ The deviations of the calculated values from the observed ones are in agreement with those published previously using LDA^{51–53} and GGA functionals.^{52,54–57} LDA underestimates the V_2O_5 equilibrium volume and c_0 by 9.1% and 10.1%, respectively, whereas GGA-PBE overestimates them by 12.3% and 11.2%, respectively. LDA and GGA-PBE yield also very different values for the (weak) bond between the V atoms and the O⁽¹⁾ oxygen of the layer beneath (cf. Table II). The LDA result is shorter than the measured value by $\sim 17\%$, whereas the GGA-PBE is larger by the same amount. As discussed before,^{56,57} the LDA and GGA-PBE deviations in the equilibrium volume and c_0 lattice constant are a consequence of the poor description of the vdW interactions between the V_2O_5 layers, which are not properly taken into account in DFT within local and gradient-corrected functionals.⁵⁸

In Fig. 2, we show the LDA and GGA-PBE potential energy surfaces of V_2O_5 as a function of the interlayer separation c for the unrelaxed (equilibrium geometry) and relaxed internal degrees of freedom, with the a and b lattice parameters held fixed at their equilibrium values, a_0 and b_0 , respectively. One can see that for both functionals, there is a minimum. We obtain with LDA an interaction energy between the V_2O_5 layers of 1.78 and 1.40 eV for the unrelaxed and relaxed geometries, respectively, whereas with GGA-PBE, we find 0.23 and 0.21 eV, respectively.

As already mentioned, the coordination of V in $CeVO_4$ is tetrahedral, which is a characteristic of all vanadate crystals. $AlVO_4$, in particular, has been recently studied in order to get insight into the nature of the Al-O-V bonds as vanadia and/or alumina catalysts possess such bonds.⁶⁰ $AlVO_4$ and $CeVO_4$ are not isostructural. The unit cell of the former is triclinic with space group $P\bar{1}$.⁶¹ The system contains two- and threefold coordinated O atoms, five- and sixfold coordinated Al atoms, and fourfold V atoms. The $AlVO_4$ structure possesses three symmetry-inequivalent VO_4 tetrahedra. The experimental V-O bond length in $CeVO_4$ of 1.71 \AA lies in the 1.62–1.84 \AA range of the values reported for $AlVO_4$ with average values of 1.72, 1.73, and 1.74 \AA for the three VO_4 tetrahedra.⁶¹

The calculated bulk modulus of $CeVO_4$ is 1.26 and 0.90 Mbar with LDA and GGA-PBE, respectively. Inclusion of the Hubbard U term yields changes of approximately -5% and $+2\%$, respectively. A similar change has been found for Ce_2O_3 in going from LDA to LDA+ U , whereas GGA-PBE+ U yields a 3% smaller value than GGA-PBE.²² For V_2O_5 , we find the usual combination of overestimated (underestimated) equilibrium volumes and underestimated (overestimated) bulk moduli, typical of GGA-PBE (LDA) (see, e.g., Ref. 43). These correlations are certainly not to be expected for $CeVO_4$ (and Ce_2O_3) in line with the underestimated equilibrium volume of $CeVO_4$ (and Ce_2O_3) by both functionals. The large difference of about 0.6 Mbar between the GGA-PBE and LDA bulk modulus for V_2O_5 is related to the strong (LDA) and weak (GGA-PBE) binding between the crystal layers (cf. Table II). The corresponding difference for CeO_2 is about 0.3 Mbar (2.01 and 1.72 Mbar for LDA and GGA-PBE, respectively).²²

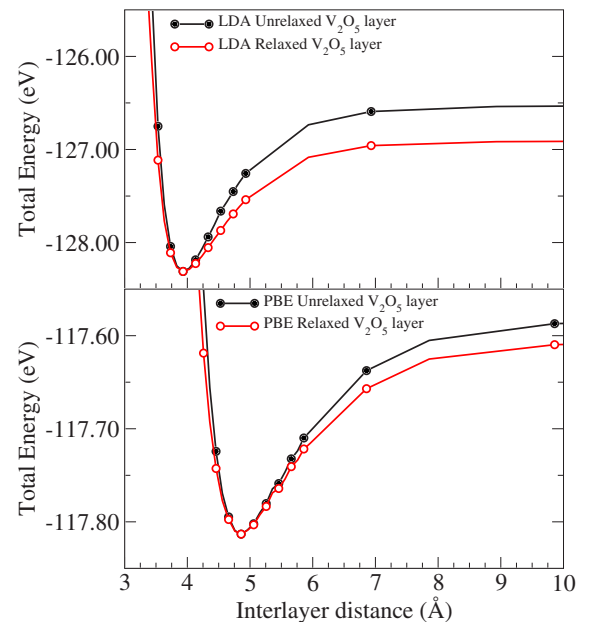


FIG. 2. (Color online) Unrelaxed and relaxed potential energy surfaces of V_2O_5 as a function of the interlayer separation between the V_2O_5 layers. a_0 and b_0 were kept fixed at their equilibrium values.

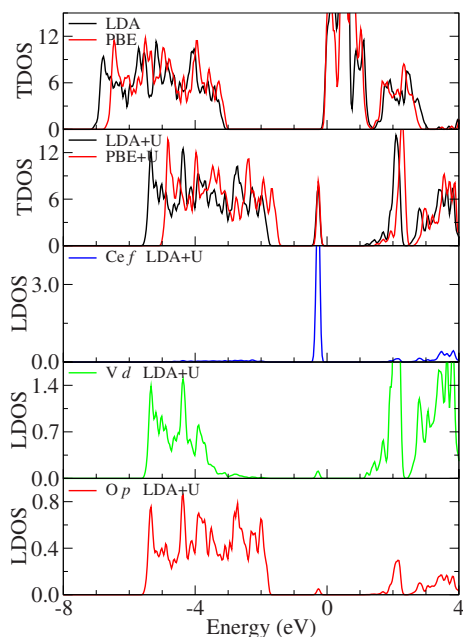


FIG. 3. (Color online) CeVO₄ total and local densities of states, TDOS and LDOS, respectively; just the main *Ce f*, *V d*, and *O p* components of the TDOS are shown. The zero energy corresponds to the top of the valence band. Only the spin-up component of the FM (AF) spin solution for LDA and GGA-PBE (LDA+*U* and GGA-PBE+*U*) is shown.

B. Magnetic and electronic properties

The total and local densities of states (DOSs) for CeVO₄ and V₂O₅ are summarized in Figs. 3 and 4, respectively. DFT+*U* yields a magnetic insulating ground state for CeVO₄, which is in agreement with experimental studies that characterized CeVO₄ as a *p*-type semiconductor by the Seebeck effect.¹⁶ However, the LDA and GGA-PBE functionals *incorrectly* predict a magnetic metallic ground state with the Fermi level intersecting the 4*f* band. Therefore, as shown by the DOS, the inclusion of the Hubbard *U* term in the LDA and GGA-PBE functionals yields a narrow (occupied) 4*f* band located about 1.0 and 1.3 eV, respectively, below the bottom of the conduction band, which is formed predominantly by V 3*d* states and Ce 5*d*+4*f* states.

DFT+*U* leads to AFM solutions that are lower in energy by 2 meV (LDA+*U*) and 1 meV (GGA-PBE+*U*) than the FM ones. As for the Ce₂O₃ system,²² the AFM and FM magnetic states are nearly degenerated in energy. The LDA and GGA-PBE functionals predict a FM metallic ground state, which is 61 meV (LDA) and 64 meV (GGA-PBE) lower in energy than the AFM solution. The occupation of the Ce 4*f* states is almost one electron per Ce atom, which gives rise to a spin magnetic moment of $\approx 1.0 \mu_B$ per Ce atom. This result is consistent with the measurement of the inverse susceptibility versus temperature of a slightly reduced sample (CeVO_{3.968}), which exhibits an AFM interaction and an effective magnetic moment of $\mu_{\text{eff}} = 1.29 \mu_B$ per Ce atom.¹⁵ For neither AFM nor FM solutions from the DFT+*U* functionals, we find *any* contribution from the V 3*d* states to the total magnetic moment. In contrast, LDA and GGA-PBE

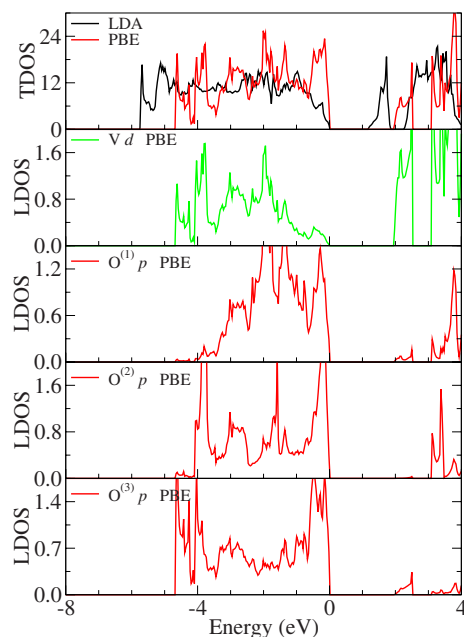


FIG. 4. (Color online) V₂O₅ total and local densities of states, TDOS and LDOS, respectively; just the main *V d* and O⁽¹⁾, O⁽²⁾, and O⁽³⁾ *p* components of the TDOS are shown. The zero energy corresponds to the top of the valence band.

predict that both the Ce 4*f* states and V 3*d* states contribute with almost 70% and 30%, respectively, to the total magnetic moment of $1.0 \mu_B$ per Ce atom of the FM ground states (see Table 1), i.e., the spin-polarized electrons are delocalized over the cerium and vanadium atoms.

As already mentioned, CeVO₄ forms upon calcination of V₂O₅/CeO₂ catalysts or during hydrocarbon oxidation reaction, and x-ray photoelectron spectroscopy⁸ and electron paramagnetic resonance measurements⁹ hinted the presence of Ce^{III+} and V^{V+}, respectively. The present DFT+*U* results for CeVO₄ support this assignment. The narrowness and occupation of the Ce 4*f* states constitute a clear proof for the localized character of these states with concomitant existence of Ce^{III+} ions.

For V₂O₅, LDA and GGA-PBE lead to a nonmagnetic insulating ground state (see Fig. 4), which is in agreement with previous theoretical studies using local and gradient-corrected functionals,^{51–53} as well as with experiment results.^{62,63} The calculated band gaps are 1.38 eV (LDA) and 2.06 eV (GGA-PBE). Experimentally, an optical band gap of ~ 2.3 eV is observed.^{62,63} We obtain the expected underestimation of band gaps using plain DFT. However, depending on the functional, there are significant differences in the size of the band gap and the width of the valence band of predominantly O 2*p* character (see Fig. 4). We ascribe these differences to the large discrepancy between the GGA-PBE and LDA results for the equilibrium volume, the interlayer spacing between the V₂O₅ layers (cf. $c_0^{\text{GGA-PBE}} - c_0^{\text{LDA}} = 0.93 \text{ \AA}$), in particular. The shorter interlayer spacing yields a larger bandwidth and a smaller band gap. LDA and GGA-PBE calculations performed for the experimental equilibrium volumes yield band gaps of 2.21 and 2.27 eV, respectively, and similar valence bandwidths of ~ 5 eV. The latter matches

well with values obtained from angle-integrated⁶⁴ and angle-resolved ultraviolet photoemission spectroscopy for crystalline V_2O_5 .⁶⁵ A closer look at the local density of states (LDOS) of the oxygen atoms labeled by $O^{(1)}$, $O^{(2)}$, and $O^{(3)}$ reveals differences, which reflect their different coordination (cf. Fig. 1), as earlier noticed.^{51–53}

C. Thermodynamic properties

The following energy differences will be discussed: (i) atomization energies E_{at} , (ii) heats of formation ΔH_f , and (iii) reaction energies ΔH_0 involved in the formation of $CeVO_4$. To calculate E_{at} , ΔH_f , and ΔH_0 and for the discussion below, the total energies E_{tot} of CeO_2 , Ce_2O_3 , V_2O_5 , VO_2 , bulk Ce, bulk V, and O_2 and the Ce, V, and O atoms are required (see the Appendix).

The total energies of the free Ce, V, and O atoms were obtained from spin-polarized calculations using an orthorhombic box ($12 \times 13 \times 14 \text{ \AA}^3$) with no constraint on the occupation of the electronic states. The total energies of CeO_2 , Ce_2O_3 , VO_2 , bulk Ce, bulk V, and O_2 were calculated employing the equilibrium parameters reported in the Appendix (Table V), which were obtained using the same procedure and computational parameters as those used for $CeVO_4$ in the present work. The equilibrium parameters reported in Table V for CeO_2 , Ce_2O_3 , bulk Ce, and O_2 are discussed elsewhere,²² whereas the structural properties of VO_2 and bulk V have been discussed early in the literature and will not be discussed in this work. For the particular case of O_2 , the atomization energy was computed using also a hard O PAW potential with a cutoff energy of 1000 eV because of the small bond distance in O_2 . In the following, when the O_2 atomization energy is used for the calculation of other energy differences, the value obtained with the hard PAW O potential is to be understood. Zero-point vibrational energy contributions and temperature effects were not included in our calculations.

1. Atomization energies and heats of formation

The Hubbard U term was added only to the Ce $4f$ states in $CeVO_4$, CeO_2 , and Ce_2O_3 , i.e., it was not added to the calculations of the free Ce atoms. Hence, the discussion of the atomization energies and heats of formation is based only on LDA and GGA-PBE results. For example, for $CeVO_4$, the atomization energy is given by the following equation:

$$E_{\text{at}}^{\text{CeVO}_4} = E_{\text{tot}}^{\text{Ce}} + E_{\text{tot}}^{\text{V}} + 4E_{\text{tot}}^{\text{O}} - E_{\text{tot}}^{\text{CeVO}_4}, \quad (1)$$

where $E_{\text{tot}}^{\text{Ce/V/O}}$ is the total energies of the free Ce, V, and O atoms, respectively, while $E_{\text{tot}}^{\text{CeVO}_4}$ is the total energy of the bulk $CeVO_4$. The atomization energies of $CeVO_4$ and V_2O_5 are summarized in Table III. The heats of formation and reaction energies, which will be discussed below, can be calculated using atomization energies; hence, we report the calculated E_{at} values for all relevant systems in Table III.

For all systems, the LDA atomization energies are larger than the GGA-PBE results, which have been commonly obtained in DFT studies (see, e.g., Refs. 43 and 66). To the best of our knowledge, experimental E_{at} values for $CeVO_4$ and V_2O_5 are not available. For bulk Ce, the GGA-PBE and

TABLE III. Atomization energies E_{at} and heats of formation ΔH_f . All results are given per f.u.

System	E_{at} (eV)		ΔH_f (eV)	
	LDA	GGA-PBE	LDA	GGA-PBE
$CeVO_4$	46.93	40.84	-19.61	-17.80
V_2O_5	50.29	43.30	-18.00	-15.70
CeO_2	24.55	21.15	-11.49	-10.36
Ce_2O_3	40.41	34.96	-18.07	-16.49
VO_2	22.50	19.22	-8.24	-6.98
Bulk Ce	5.51	4.58		
Bulk V	6.71	6.04		
O_2	7.51	6.11		
O_2^h	7.55	6.21		

LDA E_{at} values deviate by 0.26 and 1.19 eV/Ce, respectively, from the experimental value of 4.32 eV/Ce.⁶⁷ For O_2 , similar deviations from the experimental value (5.25 eV/ O_2 , Ref. 68) are obtained, namely, 0.96 (GGA-PBE) and 2.30 (LDA) eV/ O_2 . The O_2 atomization energy increases by 100 and 40 meV/ O_2 if a harder O PAW potential is used with GGA-PBE and LDA, respectively.

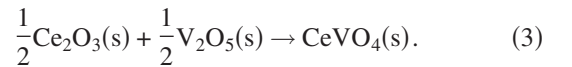
The heat of formation of $CeVO_4$, for example, is given by

$$\Delta H_f^{\text{CeVO}_4} = E_{\text{tot}}^{\text{CeVO}_4} - E_{\text{tot}}^{\text{bulk Ce}} - E_{\text{tot}}^{\text{bulk V}} - 2E_{\text{tot}}^{\text{O}_2}, \quad (2)$$

where $E_{\text{tot}}^{\text{bulk Ce/bulk V/O}_2}$ are the total energies of the bulk Ce, bulk V, and of the O_2 molecule, respectively. $\Delta H_f^{\text{CeVO}_4}$ can be calculated using the atomization energies in which $E_{\text{tot}}^{\text{bulk Ce/bulk V/O}_2}$ should be replaced by $-E_{\text{at}}^{\text{bulk Ce/bulk V/O}_2}$. The LDA and GGA-PBE heats of formation of $CeVO_4$ and V_2O_5 are summarized in Table III. As a consequence of the larger overestimation of E_{at} by LDA compared to GGA-PBE, the LDA heats of formation are also larger than the corresponding GGA-PBE results. For the case of V_2O_5 , the GGA-PBE (-15.70 eV) result is close to the experimental result of -16.07 eV,⁵⁹ while the LDA result differs by ≈ 2 eV.

2. Reaction energies

As mentioned in the Introduction, $CeVO_4$ can be synthesized by solid state reaction between Ce_2O_3 and V_2O_5 , i.e.,



The reaction energy for this reaction can be obtained by

$$\Delta H_0^{\text{Eq. (3)}} = E_{\text{tot}}^{\text{CeVO}_4} - \frac{1}{2}E_{\text{tot}}^{\text{Ce}_2O_3} - \frac{1}{2}E_{\text{tot}}^{\text{V}_2O_5}. \quad (3')$$

Another route to obtain $CeVO_4$ involves CeO_2 and V_2O_5 , i.e.,



for which the reaction energy is given by

TABLE IV. Reaction energies (ΔH_0 in eV).

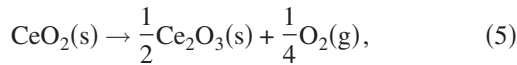
Equation No.	Reaction	LDA	GGA-PBE	LDA+ <i>U</i>	GGA-PBE+ <i>U</i>
(3)	$\frac{1}{2}\text{Ce}_2\text{O}_3 + \frac{1}{2}\text{V}_2\text{O}_5 \rightarrow \text{CeVO}_4$	-1.58	-1.71	-1.61	-1.78
(4)	$\text{CeO}_2 + \frac{1}{2}\text{V}_2\text{O}_5 \rightarrow \text{CeVO}_4 + \frac{1}{2}\text{O}_2$	+0.88	+0.41	-0.10	-0.66
(5) = (4) - (3)	$\text{CeO}_2 \rightarrow \frac{1}{2}\text{Ce}_2\text{O}_3 + \frac{1}{2}\text{O}_2$	+2.46	+2.11	+1.51	+1.12
(6)	$\frac{1}{2}\text{V}_2\text{O}_5 \rightarrow \text{VO}_2 + \frac{1}{4}\text{O}_2$	+0.76	+0.87		
(7) = (6) - (5)	$\frac{1}{2}\text{Ce}_2\text{O}_3 + \frac{1}{2}\text{V}_2\text{O}_5 \rightarrow \text{CeO}_2 + \text{VO}_2$	-1.70	-1.24	-0.75	-0.25

$$\Delta H_0^{\text{Eq. (4)}} = E_{\text{tot}}^{\text{CeVO}_4} + \frac{1}{4}E_{\text{tot}}^{\text{O}_2} - E_{\text{tot}}^{\text{CeO}_2} - \frac{1}{2}E_{\text{tot}}^{\text{V}_2\text{O}_5}. \quad (4')$$

The reaction energies are summarized in Table IV.

All functionals predict the first reaction [Eq. (3)] to be exoenergetic within a 0.2 eV energy range, which suggests a fortuitous error cancellation between the required total energies. Those of CeVO₄ and Ce₂O₃ correspond to the FM metallic and AFM insulating ground state with plain DFT and DFT+*U*, respectively. The second reaction [Eq. (4)], however, is described as endoenergetic with LDA and GGA-PBE and as exoenergetic with DFT+*U*. Note that $\Delta H_0^{\text{Eq. (4)}}$ values lie within a ~ 1.5 eV energy range.

The experimental reaction energies corresponding to Eqs. (3) and (4) are not known. However, the reduction energy of CeO₂ to Ce₂O₃, i.e.,



given by

$$\Delta H_0^{\text{Eq. 5}} = E_{\text{tot}}^{\text{Ce}_2\text{O}_3} + \frac{1}{2}E_{\text{tot}}^{\text{O}_2} - 2E_{\text{tot}}^{\text{CeO}_2}, \quad (5')$$

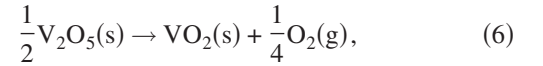
is (not very accurately) known (1.79–2.02 eV).^{69,70} $\Delta H_0^{\text{Eq. 5}}$ equals $\Delta H_0^{\text{Eq. 4}} - \Delta H_0^{\text{Eq. 3}}$ (cf. Table IV). This reaction corresponds to the cerium oxidation state change from Ce^{IV+} to Ce^{III+}.

We have recently calculated $\Delta H_0^{\text{Eq. (5)}}$ and have found that LDA and GGA-PBE overestimates the $\Delta H_0^{\text{Eq. (5)}}$ reaction energy²² by about 0.10–0.44 eV compared to the most recent experimental data (2.02 eV).⁷⁰ LDA+*U* and GGA-PBE+*U* underestimate $\Delta H_0^{\text{Eq. (5)}}$ by 0.5 eV and 0.89 eV, respectively. Thus, $\Delta H_0^{\text{Eq. (5)}}$ values (also) lie within a fairly wide energy range (~ 1.3 eV). As argued in Ref. 22, these deviations are largely related to a different description of the binding of the O₂ molecule for the LDA and GGA-PBE functionals; the relatively small deviation for the GGA-PBE case is most likely due to a fortunate cancellation of errors and not to a proper description of cerium oxides.

If we make use of the experimental value of 2.02 eV for $\Delta H_0^{\text{Eq. (5)}}$ and estimate the reaction energy between CeO₂ and V₂O₅ as $\Delta H_0^{\text{Eq. (3)}} + \Delta H_{0,\text{exp}}^{\text{Eq. (5)}}$, we obtain an endoenergetic reaction with all functionals ($\Delta H_0^{\text{Eq. (4)}} \sim 0.24$ –0.44 eV). These results, together with the discussion in Secs. III A and III B on the Ce and V oxidation state in CeVO₄, indicate that out of the two reactions between cerium oxides and vanadium

pentoxide, only the reaction is exoenergetic for which the oxidation state of Ce (and V atoms) in the reactants and product is the same, i.e., $\frac{1}{2}\text{Ce}^{\text{III+}}\text{O}_3 + \frac{1}{2}\text{V}_2^{\text{V+}}\text{O}_5 \rightarrow \text{Ce}^{\text{III+}}\text{V}^{\text{V+}}\text{O}_4$.

When V₂O₅ supported on CeO₂ is used as a catalyst in selective oxidation reactions, it is assumed that V^{V+} is reduced to V^{IV+} (or V^{III+}). The reducibility of V₂O₅ can be described by the reaction



with a reaction energy given by

$$\Delta H_0^{\text{Eq. (6)}} = E_{\text{tot}}^{\text{VO}_2} + \frac{1}{4}E_{\text{tot}}^{\text{O}_2} - \frac{1}{2}E_{\text{tot}}^{\text{V}_2\text{O}_5}. \quad (6')$$

Instead of the V^{V+} → V^{IV+} reduction, Ce^{IV+} may be reduced to Ce^{III+}, which, as already mentioned, is described by Eq. (5). The reaction



with corresponding reaction energy at zero temperature given by

$$\Delta H_0^{\text{Eq. (7)}} = E_{\text{tot}}^{\text{CeO}_2} + E_{\text{tot}}^{\text{VO}_2} - \frac{1}{2}E_{\text{tot}}^{\text{Ce}_2\text{O}_3} - \frac{1}{2}E_{\text{tot}}^{\text{V}_2\text{O}_5}, \quad (7')$$

describes the relative reducibility of CeO₂ and V₂O₅. $\Delta H_0^{\text{Eq. (7)}}$ equals $\Delta H_0^{\text{Eq. (6)}} - \Delta H_0^{\text{Eq. (5)}}$. Table IV shows that this reaction is exoenergetic with 1.70, 1.24, 0.75, and 0.25 eV for LDA, GGA-PBE, LDA+*U*, and GGA-PBE+*U*, respectively. Hence, V^{V+} is more easily reduced to V^{IV+} than Ce^{IV+} to Ce^{III+}, but the difference is small as obtained with DFT+*U*, GGA-PBE+*U*, in particular. The variation in the magnitude of this reaction energy is due to the already mentioned different performances of the various approaches for the description of the change in oxidation state of cerium, IV+ to III+. A small difference between the V^{V+} and Ce^{IV+} reducibilities such as ~ 0.2 eV may have consequences for the catalytic activity of vanadia supported on ceria. Therefore, the comparison of reactions (3) and (7) indicates that formation of the CeVO₄ phase will strongly favor the Ce^{III+}V^{V+} direction.

IV. SUMMARY

We have investigated the structural, electronic, and thermodynamic properties of CeVO₄ by DFT calculations using

TABLE V. Equilibrium parameters (in Å).

System	LDA		GGA-PBE	
	a_0	c_0	a_0	c_0
CeO ₂	5.37		5.47	
CeO ₂	5.40 ^a		5.49 ^a	
Ce ₂ O ₃	3.77	5.88	3.83	6.08
Ce ₂ O ₃	3.86 ^a	5.96 ^a	3.92 ^a	6.18 ^a
VO ₂	4.52	2.77	4.60	2.85
Bulk Ce	4.51		4.73	
Bulk V	2.93		3.00	
O ₂	1.22		1.23	
O ₂ ^h	1.21		1.22	

^aThese results were calculated with DFT+ U .

the LDA, GGA-PBE, LDA+ U , and GGA-PBE+ U functionals. V₂O₅, a reactant in the solid state reactions yielding CeVO₄,^{15,16} has also been considered in detail, whereas the other reactants, namely, CeO₂ or Ce₂O₃, were calculated using the structures reported in Ref. 22.

For CeVO₄, the equilibrium volume deviates by -2.4% (LDA+ U), $+3.6\%$ (GGA-PBE+ U), -7.4% (LDA), and -0.8% (GGA-PBE) with respect to the most recent experiments.^{13,16} DFT+ U yielded larger equilibrium volumes than DFT, which is explained as a consequence of the localization of the Ce $4f$ states in CeVO₄ with DFT+ U . Similar trends were obtained for Ce₂O₃.²² We found that the average Ce-O bond length in CeVO₄ and Ce₂O₃ are comparable and shorter by ≈ 0.15 Å than that in CeO₂. Thus, these structural similarities hint at Ce atoms having the same oxidation state in CeVO₄ and Ce₂O₃, namely, Ce^{III+}.

DFT+ U yielded an AF insulating ground state (only the Ce $4f$ states contribute to the total magnetic moments), which is in agreement with experimental observations.^{15,16} By contrast, LDA and GGA-PBE predict a FM metallic ground state. Moreover, the DFT+ U LDOS indicates that the highest occupied band is formed mainly by Ce $4f$ states, which are strongly localized. These findings resemble those for Ce₂O₃ in Ref. 22, which provides further support to our oxidation state assignment of Ce^{III+} in CeVO₄.

The structural properties of V₂O₅ are in good agreement with experimental results⁵⁰ with the exception of the interlayer distance between the V₂O₅ layers, which is largely underestimated (overestimated) by LDA (GGA-PBE). We attribute the shortcoming to the improper description of the weakly interacting V₂O₅ layers by the LDA and GGA-PBE functionals.⁵⁸

The reaction of Ce₂O₃ with V₂O₅ is predicted to be exoenergetic by all functionals ($|\Delta H_0| = 1.6\text{--}1.8$ eV). For the reaction of CeO₂ with V₂O₅, however, the different functionals yield results in a wide energy range of ~ 1.5 eV. Since the experimental energies are not known, comparison is not possible. Notably, for the CeO₂ \rightarrow $\frac{1}{2}$ Ce₂O₃ + $\frac{1}{4}$ O₂ that describes the Ce^{IV+} \rightarrow Ce^{III+} change in cerium oxidation state, a similar performance of the various functionals has been observed with LDA+ U yielding a better account for most properties.²²

TABLE VI. Total energies in eV/f.u.

System	LDA	GGA-PBE	LDA+ U	GGA-PBE+ U
CeVO ₄	-57.4698	-52.8259	-56.4640	-52.2515
CeO ₂	-28.9003	-26.2761	-26.9181	-24.6363
Ce ₂ O ₃	-47.6329	-43.3319	-45.5614	-42.0403
V ₂ O ₅	-64.1551	-58.9066		
VO ₂	-28.6902	-26.0832		
Bulk Ce	-6.8984	-5.9351		
Bulk V	-9.9380	-9.1252		
O ₂	-10.4750	-9.8785		
O ₂ ^h	-10.7213	-10.0501		
O atom	-1.4821	-1.8864		
O ^h atom	-1.5873	-1.9206		
Ce atom	-1.3872	-1.3567		
V atom	-3.2275	-3.0868		

The DFT+ U calculated structural, electronic, and thermochemical properties of CeVO₄ provide sound arguments in favor of the III+ and V+ oxidation states of Ce and V ions, respectively, and support the values inferred from experiment.^{8,9} Furthermore, we argue that the CeVO₄ phase forming in V₂O₅/CeO₂ catalysts is most likely to contain Ce^{III+} and V^{V+} cations. Thus, the present study provides an important tool for obtaining insight into the possible changes occurring to ceria supported vanadia catalysts during preparation and/or reaction.

We conclude that DFT+ U , in particular, LDA+ U , yields a better account than DFT for most of the CeVO₄ properties. It is, however, also clear that shortcomings remain, in particular, in the description of the reaction energies, which illustrates the theoretical difficulties arising from electron localization. For ceria, it has been shown that further improvements are possible with hybrid functionals that include a percentage of the exact exchange.²²

ACKNOWLEDGMENTS

This work was supported by the Deutsche Forschungsgemeinschaft (Sonderforschungsbereich 546). The calculations were carried out on the IBM pSeries 690 system of the Norddeutscher Verbund für Hoch- und Höchstleistungsrechnen (HLRN).

APPENDIX

Table V summarizes the equilibrium parameters of CeO₂ (fluorite type, $Fm\bar{3}m$), Ce₂O₃ (sesquioxide A type, $P\bar{3}m1$), VO₂ (rutile), bulk Ce (face-centered cubic), bulk V (body-centered cubic), and of the O₂ molecule, which were employed in the total energy calculations required in Sec. III. The respective total energies are summarized in Table VI. They were obtained using standard PAW potentials provided within VASP and 400 eV for the cutoff energy, except for the O₂^h and O^h, which were calculated using hard PAW and oxygen PAW potentials and 1000 eV for the cutoff energy.

- *Present address: National Renewable Energy Laboratory, 1617 Cole Blvd., Golden, CO 80401; juarez_dasilva@nrel.gov
†vgp@chemie.hu-berlin.de
‡js@chemie.hu-berlin.de
- ¹B. M. Weckhuysen and D. E. Keller, *Catal. Today* **78**, 25 (2003).
 - ²A. Khodakov, B. Olthof, and A. T. Bell, *J. Catal.* **181**, 205 (1999).
 - ³M. A. Bañares, M. V. Martínez-Huerta, X. Gao, J. L. G. Fierro, and I. E. Wachs, *Catal. Today* **61**, 295 (2000).
 - ⁴I. E. Wachs, *Catal. Today* **100**, 79 (2005).
 - ⁵J. M. Vohs and G. S. Wong, *Catal. Today* **85**, 303 (2003).
 - ⁶T. Feng and J. M. Vohs, *J. Catal.* **221**, 619 (2004).
 - ⁷W. Daniell, A. Ponchel, S. Kuba, F. Anderle, T. Weingand, D. H. Gregory, and H. Knözinger, *Top. Catal.* **20**, 65 (2002).
 - ⁸B. M. Reddy, A. Khan, Y. Yamada, T. Kobayashi, S. Loridant, and J.-C. Volta, *J. Phys. Chem. B* **107**, 5162 (2003).
 - ⁹M. V. Martínez-Huerta, J. M. Coronado, M. Fernández-García, A. Iglesias-Juez, G. Deo, J. L. G. Fierro, and M. A. Bañares, *J. Catal.* **225**, 240 (2004).
 - ¹⁰R. L. Jones and C. E. Willians, *Surf. Coat. Technol.* **32**, 349 (1987).
 - ¹¹G. Picardi, F. Varsano, F. Decker, U. Opara-Krasovec, A. Surca, and B. Orel, *Electrochim. Acta* **44**, 3157 (1999).
 - ¹²U. O. Kračovec, B. Orel, A. Šurca, N. Bukovec, and R. Reisfeld, *Solid State Ionics* **118**, 195 (1999).
 - ¹³E. V. Tsipis, M. V. Patrakeev, V. V. Kharton, N. P. Vyshatko, and J. R. Frade, *J. Mater. Chem.* **12**, 3738 (2002).
 - ¹⁴L. H. Brixner and E. Abramson, *J. Electrochem. Soc.* **112**, 70 (1965).
 - ¹⁵M. Yoshimura and T. Sata, *Bull. Chem. Soc. Jpn.* **42**, 3195 (1969).
 - ¹⁶A. Watanabe, *J. Solid State Chem.* **153**, 174 (2000).
 - ¹⁷H. Wang, Y.-Q. Meng, and H. Yan, *Inorg. Chem. Commun.* **7**, 553 (2004).
 - ¹⁸F. Luo, C.-J. Jia, W. Song, L.-P. You, and C.-H. Yan, *Cryst. Growth Des.* **5**, 137 (2005).
 - ¹⁹A. Trovarelli, *Catal. Rev. - Sci. Eng.* **38**, 439 (1996).
 - ²⁰R. F. Reidy and K. E. Swider, *J. Am. Ceram. Soc.* **78**, 1121 (1995).
 - ²¹F. W. Kutzler, D. E. Ellis, D. J. Lam, B. W. Veal, A. P. Paulikas, A. T. Aldred, and V. A. Gubanov, *Phys. Rev. B* **29**, 1008 (1984).
 - ²²J. L. F. Da Silva, M. V. Ganduglia-Pirovano, J. Sauer, V. Bayer, and G. Kresse, *Phys. Rev. B* **75**, 045121 (2007).
 - ²³P. Hohenberg and W. Kohn, *Phys. Rev.* **136**, B864 (1964).
 - ²⁴W. Kohn and L. J. Sham, *Phys. Rev.* **140**, A1133 (1965).
 - ²⁵J. P. Perdew and Y. Wang, *Phys. Rev. B* **45**, 13244 (1992).
 - ²⁶J. P. Perdew, K. Burke, and M. Ernzerhof, *Phys. Rev. Lett.* **77**, 3865 (1996).
 - ²⁷V. I. Anisimov, J. Zaanen, and O. K. Andersen, *Phys. Rev. B* **44**, 943 (1991).
 - ²⁸C. Loschen, J. Carrasco, K. M. Neyman, and F. Illas, *Phys. Rev. B* **75**, 035115 (2007).
 - ²⁹D. A. Andersson, S. I. Simak, B. Johansson, I. A. Abrikosov, and N. V. Skorodumova, *Phys. Rev. B* **75**, 035109 (2007).
 - ³⁰M. V. Ganduglia-Pirovano, A. Hofmann, and J. Sauer, *Surf. Sci. Rep.* **62**, 219 (2007).
 - ³¹S. L. Dudarev, G. A. Botton, S. Y. Savrasov, C. J. Humphreys, and A. P. Sutton, *Phys. Rev. B* **57**, 1505 (1998).
 - ³²S. Fabris, S. de Gironcoli, S. Baroni, G. Vicario, and G. Balducci, *Phys. Rev. B* **72**, 237102 (2005).
 - ³³M. Cococcioni and S. de Gironcoli, *Phys. Rev. B* **71**, 035105 (2005).
 - ³⁴P. E. Blöchl, *Phys. Rev. B* **50**, 17953 (1994).
 - ³⁵G. Kresse and D. Joubert, *Phys. Rev. B* **59**, 1758 (1999).
 - ³⁶O. Bengone, M. Alouani, P. Blöchl, and J. Hugel, *Phys. Rev. B* **62**, 16392 (2000).
 - ³⁷G. Kresse and J. Hafner, *Phys. Rev. B* **48**, 13115 (1993).
 - ³⁸G. Kresse and J. Furthmüller, *Phys. Rev. B* **54**, 11169 (1996).
 - ³⁹H. J. Monkhorst and J. D. Pack, *Phys. Rev. B* **13**, 5188 (1976).
 - ⁴⁰F. D. Murnaghan, *Proc. Natl. Acad. Sci. U.S.A.* **50**, 697 (1944).
 - ⁴¹C. Baudracco-Gritti, S. Quartieri, G. Vezzalini, F. Permingeat, F. Pillard, and R. Rinaldi, *Bull. Mineral.* **110**, 657 (1987).
 - ⁴²M. Fuchs, J. L. F. Da Silva, C. Stampfl, J. Neugebauer, and M. Scheffler, *Phys. Rev. B* **65**, 245212 (2002).
 - ⁴³J. L. F. Da Silva, C. Stampfl, and M. Scheffler, *Surf. Sci.* **600**, 703 (2006).
 - ⁴⁴S. J. Duclos, Y. K. Vohra, A. L. Ruoff, A. Jayaraman, and G. P. Espinosa, *Phys. Rev. B* **38**, 7755 (1988).
 - ⁴⁵L. Gerward and J. S. Olsen, *Powder Diffr.* **8**, 127 (1993).
 - ⁴⁶A. Nakajima, A. Yoshihara, and M. Ishigame, *Phys. Rev. B* **50**, 13297 (1994).
 - ⁴⁷L. Gerward, J. S. Olsen, L. Petit, G. Vaitheeswaran, V. Kanchana, and A. Svane, *J. Alloys Compd.* **400**, 56 (2005).
 - ⁴⁸H. Pinto, M. H. Mintz, M. Melamud, and H. Shaked, *Phys. Lett.* **88A**, 81 (1982).
 - ⁴⁹H. Bärnighausen and G. Schiller, *J. Less-Common Met.* **110**, 385 (1985).
 - ⁵⁰R. Enjalbert and J. Galy, *Acta Crystallogr., Sect. C: Cryst. Struct. Commun.* **42**, 1467 (1986).
 - ⁵¹V. Eyert and K.-H. Höck, *Phys. Rev. B* **57**, 12727 (1998).
 - ⁵²X. Yin, A. Fahmi, A. Endou, R. Misura, I. Gunji, R. Yamauchi, M. Kubo, A. Chatterjee, and A. Miyamoto, *Appl. Surf. Sci.* **130**, 539 (1998).
 - ⁵³A. Chakrabarti, K. Hermann, R. Druzinic, M. Witko, F. Wagner, and M. Petersen, *Phys. Rev. B* **59**, 10583 (1999).
 - ⁵⁴J. S. Braithwaite, C. R. A. Catlow, J. D. Gale, and J. H. Harding, *Chem. Mater.* **11**, 1990 (1999).
 - ⁵⁵G. Kresse, S. Surnev, M. G. Ramsey, and F. P. Netzer, *Surf. Sci.* **492**, 329 (2001).
 - ⁵⁶V. Brázdová, M. V. Ganduglia-Pirovano, and J. Sauer, *Phys. Rev. B* **69**, 165420 (2004).
 - ⁵⁷M. V. Ganduglia-Pirovano and J. Sauer, *Phys. Rev. B* **70**, 045422 (2004).
 - ⁵⁸H. Rydberg, M. Dion, N. Jacobson, E. Schröder, P. Hyldgaard, S. I. Simak, D. C. Langreth, and B. I. Lundqvist, *Phys. Rev. Lett.* **91**, 126402 (2003).
 - ⁵⁹*NIST Chemistry WebBook*, edited by P. J. Linstrom and W. G. Mallard (National Institute of Standards and Technology, Gaithersburg, MD, 2001), <http://webbook.nist.gov>.
 - ⁶⁰V. Brázdová, M. V. Ganduglia-Pirovano, and J. Sauer, *J. Phys. Chem. B* **109**, 394 (2005).
 - ⁶¹E. Arisi, S. A. Palomares Sánchez, F. Leccabue, B. E. Watts, G. Bocelli, F. Calderón, G. Calestani, and L. Righi, *J. Mater. Sci.* **39**, 2107 (2004).
 - ⁶²N. Kenny, C. R. Kannerwurf, and D. H. Whitmore, *J. Phys. Chem. Solids* **27**, 1237 (1966).
 - ⁶³Z. Bodó and I. Hevesi, *Phys. Status Solidi* **20**, K45 (1967).
 - ⁶⁴S. Shin, S. Suga, M. Taniguchi, M. Fujisawa, H. Kanzaki, A. Fujimori, H. Daimon, Y. Ueda, K. Kosuge, and S. Kachi, *Phys. Rev. B* **41**, 4993 (1990).

- ⁶⁵B. Tepper, B. Richter, A. C. Dupuis, H. Kuhlenbeck, C. Hucho, P. Schilbe, M. A. bin Yarmo, and H. J. Freund, *Surf. Sci.* **496**, 64 (2002).
- ⁶⁶J. Paier, M. Marsman, K. Hummer, G. Kresse, I. C. Gerber, and J. G. Ángyán, *J. Chem. Phys.* **124**, 154709 (2006).
- ⁶⁷C. Kittel, *Introduction to Solid State Physics*, 7th ed. (Wiley, New York, 1996).
- ⁶⁸G. Herzberg, *Molecular Spectra and Molecular Structure I: Spectra of Diatomic Molecules*, 2nd ed. (Krieger, Melbourne, FL, 1989).
- ⁶⁹A. Trovarelli, *Catalysis by Ceria and Related Materials*, 1st ed. (World Scientific, Singapore, 2002).
- ⁷⁰M. Zinkevich, D. Djurovic, and F. Aldinger, *Solid State Ionics* **177**, 989 (2006).